Journal of Exposure Analysis and Environmental Epidemiology **(1999) 9, 322–335**

http://www.stockton-press.co.uk

A study of the spatiotemporal health impacts of ozone exposure

GEORGE CHRISTAKOS AND ALEXANDER KOLOVOS

Environmental Modelling Program, Department of Environmental Sciences and Engineering, School of Public Health, CB#7400, School of Public Health, University of North Carolina at Chapel Hill, Chapel Hill, North Carolina

Exposure analysis and mapping of spatiotemporal pollutants in relation to their health effects are important challenges facing environmental health scientists and integrated assessment modellers. In this work, a methodological framework is discussed to study the impact of spatiotemporal ozone (O_3) exposure distributions on the health of human populations. The framework, however, is very general and can be used to study various other pollutants. The spatiotemporal analysis starts with exposure distributions producing the input to pollutokinetic (or toxicokinetic) laws which are linked to effect models which, in turn, are integrated with relationships that describe how effects are distributed across populations. Important characteristics of the environmental health framework are holisticity and stochasticity. Holisticity emphasizes the functional relationships between composite space/time O_3 maps, pollutokinetic models of burden on target organs and tissues, and health effects. These relationships offer a meaningful physical interpretation of the exposure and biological processes that affect human exposure. Stochasticity involves the rigorous representation of natural uncertainties and biological variations in terms of spatiotemporal random fields. The stochastic perspective introduces a deeper epistemological understanding in the development of improved models of spatiotemporal human exposure analysis and mapping. Also, it explicitly determines the knowledge bases available and develops logically plausible rules and standards for data processing and human exposure map construction. The proposed approach allows the horizontal integration among sciences related to the human exposure problem that leads to accurate and informative spatiotemporal maps of O_3 exposure and effect distributions and an integrative analysis of the whole risk case. By processing a variety of knowledge bases, the spatiotemporal analysis can bring together several sciences which are all relevant to the aspect of human exposure reality that is examined.

Keywords: *burden, epistemology, exposure, health effect, ozone, stochastic analysis.*

Introduction

This paper presents a general method for studying the health effects of pollutants distributed in space and time. The method is then implemented to study ozone (O_3) concentration levels over eastern US. Ozone is photochemically produced from the combination of volatile organic compounds and oxides of nitrogen in the presence of sunlight. Human exposure to high levels of O_3 can have acute as well as chronic health effects (McDonnell et al., 1983; Thurston et al., 1992; McCurdy, 1994). Ozone levels have become high enough over eastern US during the summer period to cause significant damage to crops and vegetation. The O_3 data set considered in this study includes ambient O_3 concentration observations from the Aerometric Information Retrieval System (AIRS) maintained by the US Environmental Protection Agency (USEPA).

1. Address all correspondence to: George Christakos, Environmental Modelling Program, Department of Environmental Sciences and Engineering, School of Public Health, CB#7400, School of Public Health, University of North Carolina at Chapel Hill, Chapel Hill, NC 27599-7400. Tel.: (919)966-1767. Fax: (919)966-7911. E-mail: george_christakos@unc.edu

Exposure generally refers to the contact of a receptor with the environmental pollutant. Usually, exposure is considered equal to the airborne pollutant concentration at a specific point in space and time. Exposure concentration, however, does not represent the amount of the pollutant that accumulates in a target organ (i.e., an organ in which the important damage will occur), for it ignores the biokinetic and transformation properties of the pollutant in the body (Leung, 1991; Schulte and Perera, 1993). The amount of O_3 in the body that can exhibit harmful effects on a target organ (e.g., lung) is denoted by an appropriate biological exposure variable (leading to the definition of the so-called pollutant biomarkers), which is not necessarily strictly proportional to the exposure concentration (Christakos and Hristopulos, 1998). The main biological exposure variable considered in this work is burden, which provides a measure of the fraction of the inhaled pollutant that reaches target organs and tissues of the receptor and is capable of affecting them. Studies have shown that O_3 burden and receptor response are correlated, and a knowledge of O_3 burden is prerequisite to an unambiguous evaluation of health effects (Hu et al., 1992). The burden is calculated from the toxicokinetic (or pollutokinetic) equations, which take into consideration exposure variations in space/time as well as variabilities linked to the biological and physiological characteristics of

the individual. As a result, these equations can provide information about the functional relationship between exposure and burden, which is essential in the evaluation of the assumptions underlying the health response models and the assessment of the actual damage on human populations due to O_3 exposure. It is worth-mentioning that in some exposure studies, burden is considered synonymous to dose. In modern human health practice, however, burden is defined8063 as above, while the term 'dose' refers to the interaction rate between the biologically active form and target organs in the receptor (Crawford-Brown, 1997).

Due to the considerable physical uncertainty (caused by physiographic characteristics, emission fluctuations, meteorological conditions, etc.) and biological variability linked to the individual (pulmonary ventilation, body build, etc.), the exposure distribution and the biological variables are represented in terms of spatiotemporal random fields (S/TRF; Christakos, 1992). The S/TRF domain is a space/time continuum, in which space represents the order of coexistence and time represents the order of successive existence. Specification of the O_3 exposure values at all points in a space/time continuum specifies a realization of the S/TRF. Randomness manifests itself as an ensemble of possible realizations regarding the distribution of the exposure and biological variables.

All of the many questions about O_3 health hazards divide into three lines of investigation: define the exposure conditions; relate exposure to burden in the body; and detect adverse health effects and estimate population damages. In this work, an efficient stochastic approach is discussed for quantifying these lines of investigation. This approach has three main parts as follows (see also Figure 1; the precise meaning of the various symbols used in the figure will become clear later in the text).

(a) Random field modelling can produce accurate O_3 exposure (E) maps in space/time, given the knowledge bases ($\mathcal{K}$) available. An appealing feature of the mapping approach is that it is mathematically rigorous as well as epistemologically meaningful.

(b) From physiological, biochemical, metabolic, etc., data, the appropriate pollutokinetic equations can be developed and solved to obtain the O_3 burden (B) map.

(c) The burden map is inserted into the probabilistic health response and damage models to estimate the expected health effect (H) on a receptor, as well as the population damage (Ψ_v and ψ_v) due to O_3 exposure.

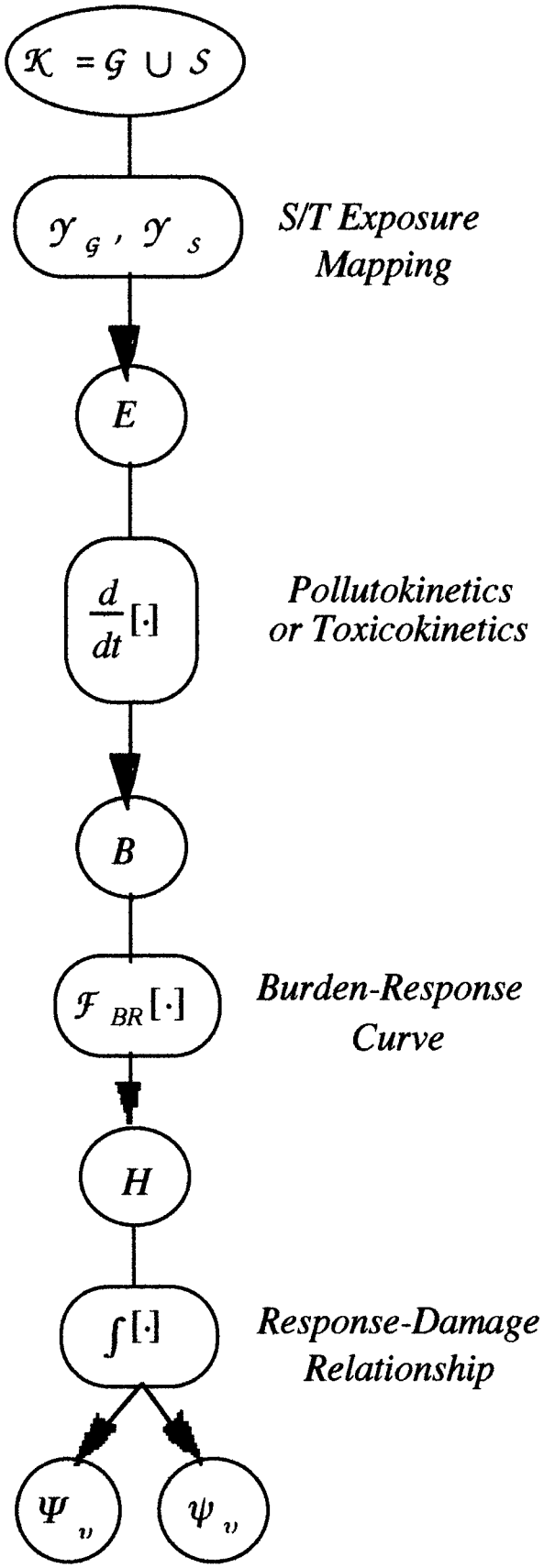

Figure 1. An approach for studying the effects of O_3 exposure on human populations $\mathcal{K}$ = knowledge bases ($\mathcal{G}$ = general knowledge and $\mathcal{S}$ = specificatory knowledge), $\mathcal{Y}_{\mathcal{G}}$ and $\mathcal{Y}_{\mathcal{S}}$ = knowledge processing operators, E = exposure map, B = burden on receptor, H = health effect, Ψ_v and ψ_v = population damage indicators.

The approach above introduces a holistic perspective that looks at the whole picture of human exposure assessment: pollutant exposure and subsequent burden on the receptor, health effects, and population damages. Each part of the approach incorporates knowledge from a variety of sources. The data used in part (a) are obtained from air monitoring, in part (b) from biologic monitoring, and in part (c) from health damage surveillance. These data are assumed to vary within a domain that integrates space and time (neither space nor time are fixed and can vary simultaneously). The approach offers a sound physical interpretation of the exposure and biological processes affecting human health, and takes into account the uncertainty present in the observation of these processes and the usually imperfect knowledge bases available. It provides graphical information about the composite space/time exposure pattern, which is a considerable improvement over previous studies based on purely spatial data analysis. Rigorous expressions of the burden variability can be obtained in terms of the exposure variation and the biologic properties of the receptors, which have significant advantages over commonly used statistics of individual receptor cases. Collectively, these capabilities of the human exposure approach provide the means to enhance individual and group health risk assessments. In the following sections we will discuss in detail the various parts of Figure 1.

BME exposure mapping

Various methods can be implemented to construct maps of human exposure variables in space/time. Among other things, a useful mapping approach should explain when and how one can cope rationally with the uncertainty of exposure and biological variables. The Bayesian maximum entropy approach (BME; Christakos, 1992) achieves such a task by a fruitful combination of three basic elements: the S/TRF model, the knowledge bases available, and a sound epistemological framework. More specifically, the variables of interest are represented in terms of S/TRFs, which offer a general framework for analyzing human exposure data distributed in space/time. Various knowledge bases can be used in human exposure analysis (e.g., general and specificatory knowledge bases). From an epistemological viewpoint, spatiotemporal mapping is a combination of both the examination of hypotheses regarding human exposure and the determination of estimates for the values of the exposure and the biological variables involved.

Natural theories parameterized by space and time variables are considered more basic than those that are not. Human exposure mapping in a space/time continuum (i.e., a continuous spatial arrangement combined with a temporal order of events) involves two separate entities: spatial coordinates $\boldsymbol{s}=(s_1,s_2)$ considered in the Euclidean space R^2 and a temporal coordinate t along the time axis T. The coordinates $(\boldsymbol{s},t)$ are defined on the Cartesian product $R^2\times T$. An exposure S/TRF $E(\boldsymbol{p})$ is a collection of field realizations ε associated with the exposure values at the points $\boldsymbol{p}=(\boldsymbol{s},t)$ of the space/time continuum; each realization has a probability of occurrence denoted by $P(\varepsilon)$. Mathematically rigorous definition of the S/TRF may be found in Christakos (1992).

Viewing them separately, space and time are both continua and, thus, they share all the properties that the abstract notion of continuum possesses in general. But time also has certain extra-continua physical properties, which it does not share with any other continuum (e.g., recursivity is an extra-continua property of time, but not of space); the same is true of space. When space and time are brought together, the extra-continua physical properties of space integrate with those of time, producing a holistic space/time in which the whole is greater than the sum of its parts. In such a holistic environment, spatiotemporal connections and cross-effects may control physical and biological variations.

A system of pure axiomatic geometry does not suffice, if geometry is to be applied to the natural space/time. What is required is to establish a relation between the geometric concepts of the abstract system with the natural processes of the environmental system. To establish such a relation, one must take into consideration the fact that, while mathematical geometry is purely logical, physical geometry is empirical. In other words, the empirical investigation of space/time as a whole (including all forms of physical knowledge $\mathcal{K}$ available) should disclose the nature of the mathematical geometry that best describes it. Consider, e.g., a point P in $R^2\times T$ with space/time coordinates $\boldsymbol{p}=(s_1,s_2,t)$, so that an exposure S/TRF varying within this continuum is written as $E(\boldsymbol{p})=E(s_1,s_2,t)$ (Figure 2). The wavy line denotes that the space/time vector $\overrightarrow{OP}=\boldsymbol{p}$ may not, in general, have the usual Euclidean metrical structure. In order to determine a suitable spatiotemporal metric, the physical knowledge $\mathcal{K}$ available about $E(\boldsymbol{p})$ may need to be taken into consideration. An example is discussed in Appendix A.

The total knowledge $\mathcal{K}$ used in human exposure analysis may include all kinds of valid knowledge that are available at a given moment and can be obtained by the competent scientist using effectively a scientific procedure. One may distinguish between two prime bases of knowledge: the general knowledge base $\mathcal{G}$ (general in the sense that it is vague enough to characterize a large class of exposure situations), and the specificatory (or case-specific) knowledge base $\mathcal{S}$ (i.e., knowledge about the specific situation). The union of $\mathcal{G}$ and $\mathcal{S}$ is the total knowledge $\mathcal{K}=\mathcal{G}\cup\mathcal{S}$.

More specifically, $\mathcal{G}$ may include physical and biological laws, logical relations, statements of fact, and theories. In many cases, it is useful to establish a mathematical

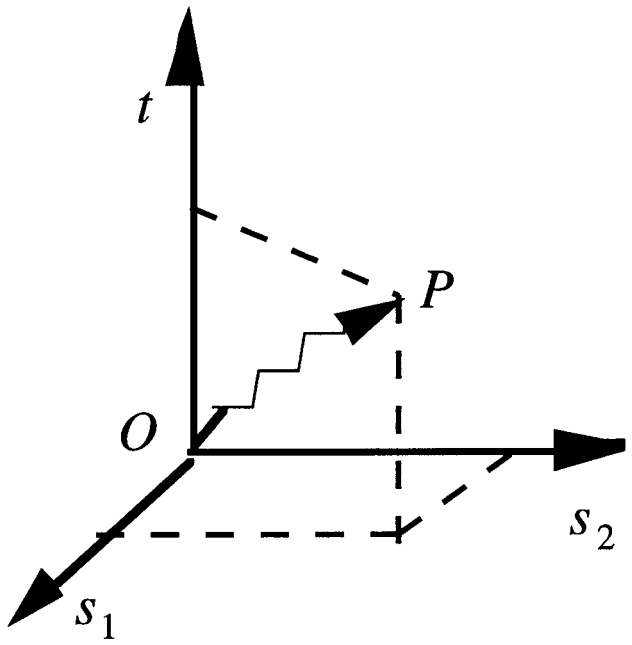

Figure 2. A point in the space–time domain $R^2 \times T$.

formulation of $\mathcal{G}$ in terms of a series of functions of the exposure realizations ε, i.e., $\mathcal{G}$: $g_\alpha(\varepsilon)$, $\alpha=0,1,\ldots,N_c$. Criteria involved in the choice of the g_α's include the requirement that the stochastic expectations $\overline{g}_\alpha$ be calculable and that the resulting equations be solvable with respect to the unknown parameters. For illustration, consider the simple case $g_1(\varepsilon)=\varepsilon$; then $\overline{g}_1 = \overline{E}$ is the mean exposure. Similarly, if $g_2(\varepsilon) = (\varepsilon - \overline{E})^2$, the $\overline{g}_2 = \sigma_E^2$ is the exposure variance. Data sets $\varepsilon_{\text{data}}$ available as specificatory knowledge $\mathcal{S}$ are usually divided into two main groups as follows. $\mathcal{S}$: $\varepsilon_{\text{data}} = (\varepsilon_{\text{hard}}, \varepsilon_{\text{soft}}) = (\varepsilon_1, \ldots, \varepsilon_m)$, where $\varepsilon_{\text{hard}}$ denotes hard data and $\varepsilon_{\text{soft}}$ denotes soft data. Hard data are measurements obtained from real-time observation devices, experiments on human subjects and nonhuman organisms, etc. The soft data may represent varying levels of understanding of uncertain observations leading to the direct calculation of the probabilities or their indirect estimation from accumulated experience (Christakos, 1998a and 1998b).

Spatiotemporal exposure mapping seeks estimates $\hat{\varepsilon}_\ell$ of an exposure S/TRF $E(\boldsymbol{p})$ at certain points $\boldsymbol{p}_\ell \in R^2 \times T$ given general knowledge and case-specific data. In most applications, the $\boldsymbol{p}_\ell$ are unsampled points that lie on the nodes of a space/time grid. Technically, one may distinguish between spatial, temporal, and spatiotemporal exposure maps, depending upon whether they capture a single instantaneous snapshot (i.e., a picture), a sequence of successive snapshots at a single geographical location (a time profile), or a video sequence of successive spatial pictures (i.e., a movie). While single-point mapping deals with one estimate $\hat{\varepsilon}_\ell$ at a time, multi-point mapping is concerned with several interdependent estimates $\hat{\boldsymbol{\varepsilon}}_\ell = (\hat{\varepsilon}_{\ell_1}, \hat{\varepsilon}_{\ell_2}, \ldots)$ simultaneously. BME focuses on levels of human exposure analysis as they relate to understanding: The spatiotemporal mapping of human exposure variables should be both informative (*a priori* information maximization given $\mathcal{G}$) and cogent (*a posteriori* probability maximization given $\mathcal{S}$). This double epistemological goal produces estimates $\hat{\varepsilon}_\ell$ with the highest probability (mode estimates), which are computed directly as solutions of the BME exposure equations presented in Appendix A, Equations A.1 and A.2. Mean exposure estimates, percentiles, etc., are also obtained from the *a posteriori* probability density function (pdf) of Equation A.3. There are two fundamental operators involved in Equations A.1–A.3: the $\mathcal{Y}_\mathcal{G}$-operator that incorporates general knowledge $\mathcal{G}$, and the $\mathcal{Y}_\mathcal{S}$-operator that incorporates specificatory knowledge $\mathcal{S}$. The operators can represent objective and subjective forms of knowledge available in exposure assessment (several of these forms are discussed in Taylor, 1993). Explicit mathematical expressions for $\mathcal{Y}_\mathcal{G}$ and $\mathcal{Y}_\mathcal{S}$ are available in the literature for a wide range of applications (Choi et al., 1998; Christakos, 1998a and 1998b; Serre et al., 1998; references therein).

BME not only satisfies sound epistemological ideals and incorporates physical knowledge bases in a rigorous and systematic manner, but it also has certain other attractive features. It does not require any assumption regarding the shape of the underlying probability law (hence, non-Gaussian laws are automatically incorporated). It leads to nonlinear estimators, in general, and can model nonhomogeneous/nonstationary human exposure data. It is easily extended to functional and vector exposure variables. Depending upon the knowledge bases $\mathcal{G}$ and $\mathcal{S}$ considered, many existing mapping techniques can be derived as special cases of the BME approach. For example, by considering up to second-order statistical moments and hard data only, the space/time mapping method discussed in Christakos and Vyas (1998a and 1998b) can be derived from Equation A.1 and A.2 of Appendix A. Geostatistical kriging is a special case of BME. BME, also, leads to novel and more general results that could not be obtained with traditional mapping analysis.

In the following study, the specificatory knowledge $\mathcal{S}$ consists of the O_3 data set provided by the AIRS–USEPA. This data set includes 1228 monitoring stations east of 95° west longitude and north of 25° north latitude. At each monitoring station, 1-h O_3 concentration observations are available which are considered as the 1-h O_3 exposure $E_{1\text{-h}}(\boldsymbol{p})$, in parts per million, at the space/time point $\boldsymbol{p}=(s,t)$. At this point, it might be appropriate to notice that, while O_3 concentration refers to a physical point $\boldsymbol{p}$ per se, O_3 exposure is associated with a receptor located at the point $\boldsymbol{p}$ (in the following, both interpretations of $\boldsymbol{p}$ will be used). Widespread air pollution episodes observed during the summer months are related to chemical processes and

meteorological conditions that facilitate the photochemical production of O_3 (Logan, 1989). At each geographical location, the temporally averaged 1-h O_3 exposure $E(\boldsymbol{p})$ is calculated from Equation B.1 of Appendix B. As is shown in Equation B.1, the $E(\boldsymbol{p})$ is a function of the exposure duration τ_e (in hours) during each day, and the exposure frequency f_e (in percentage), i.e., the fraction of total exposure time during which the person is actually exposed. Therefore, calculation of the exposure field $E(\boldsymbol{p})$ requires information about the space/time O_3 distribution, the exposure duration, and the exposure frequency. This leads to a physical basis established by means of the space/time domain $(\boldsymbol{p},\tau_e)$ containing the pollutant. The τ_e and f_e may play an important role in the assessment of potential health effects (e.g., while exposure from lower O_3 concentrations over long time periods produces no harmful effects on sensitive receptors, the same total exposure delivered over short duration at high levels can produce respiratory problems; Ryan, 1991). The general knowledge $\mathcal{G}$ available about the O_3 distribution is that the distribution is characterized by nonhomogeneous spatial patterns, nonstationary temporal trends, and random local fluctuations. As a consequence, O_3 exposure is represented in terms of the S/TRF-ν/μ model with a generalized spatiotemporal covariance of the form of Equation C.1 in Appendix C. Equation C.1 takes into consideration correlations and dependencies of exposure values between different points in space/time.

On the basis of these two knowledge bases $\mathcal{G}$ and $\mathcal{S}$, the mapping Equation A.1 and Equation A.2 of Appendix A can be solved to provide O_3 exposure estimates at any point in space/time where observations are not available. The average O_3 exposure $E(\boldsymbol{p})$ during each day (i.e., τ_e=24 h in Equation B.1 of Appendix B) was calculated for a geographical region in eastern US that includes New York City and Philadelphia. While such an averaging could smooth out high peaks in the 1-h O_3 profiles and, thus, may not be appropriate to ascertain compliance with certain ambient air quality standards (which was the goal of earlier studies; Christakos and Vyas, 1998a), it is nevertheless appropriate for the biological indicator and health effect analysis of the present work. In Figure 3, spatial exposure maps are plotted for a few selected days in July of 1995. These maps can help us detect variations in the daily-averaged O_3 exposure across areas and identify spatiotem-

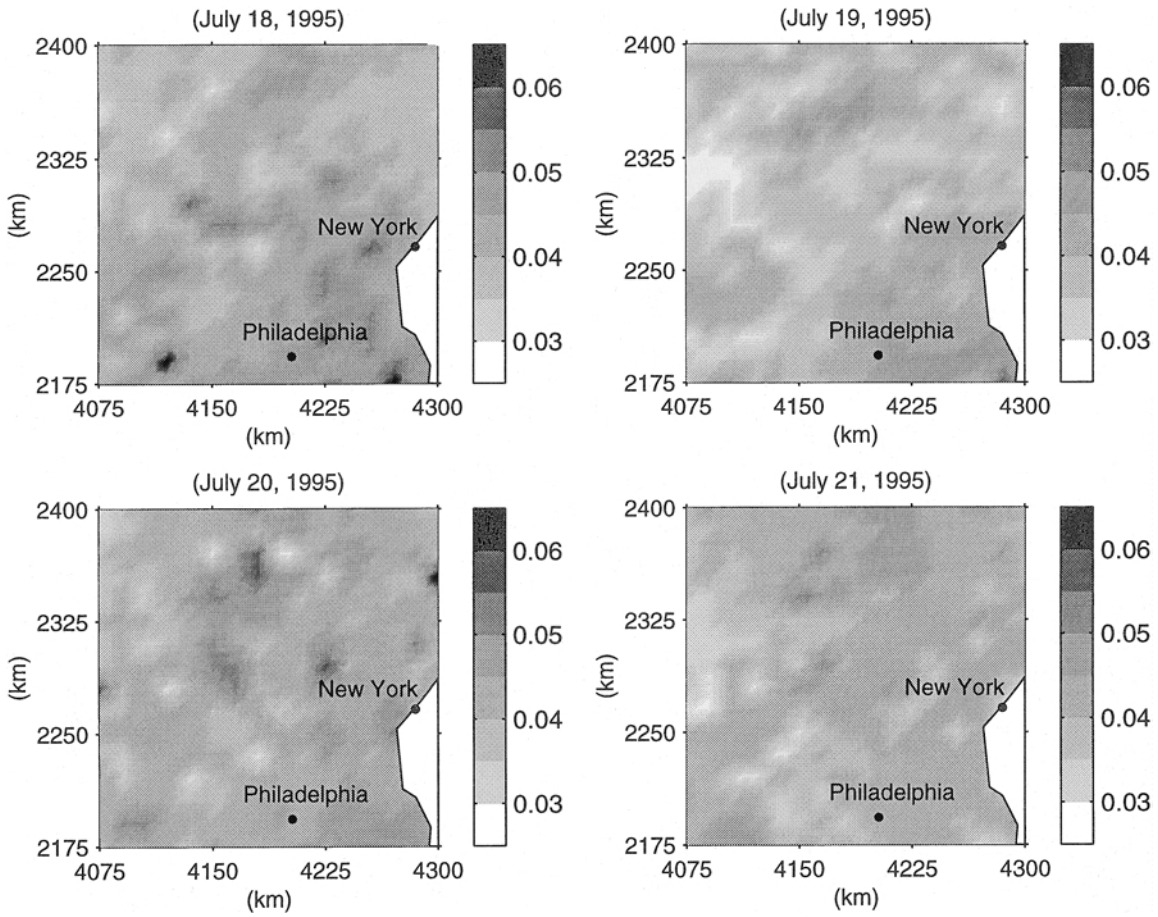

Figure 3. Daily-averaged O_3 exposure maps (ppm) at a region of eastern US.

poral exposure patterns of considerable importance in health studies (trends, etc.). Certain differences between spatial and temporal exposure variations may be due to extra-continua properties of space and time, topographic characteristics of the region, urban activities, meteorological conditions, etc. The exposure maps honor the data values at points in which monitoring stations exist. Moreover, the associated histograms of the estimation error variances at unsampled points—not plotted here—demonstrated the very good accuracy of the space/time O_3 exposure maps.

Pollutokinetic or toxicokinetic modelling

As is depicted in the outline of the human exposure approach (Figure 1), there exist important links between O_3 exposure and subsequent burden, health effect, and population damage. The first link requires that O_3 exposure variations be transformed efficiently into burden (which is the important variable, for it has a more direct connection with potential health effects than airborne O_3 concentration). The transformation can be made by means of pollutokinetic (or toxicokinetic) models that predict burden distributions in the human organs and tissues, resulting from exposure to pollutants. The terms 'pollutokinetics' or 'toxicokinetics' are similar to the term 'pharmacokinetics' which is the study of the rate of change in drug and metabolite concentration in the body. Pollutokinetic modelling typically involves compartmental models, which are particularly useful in the study of transfer and transformation processes that occur in the body following exposure to a pollutant (Piotrowski, 1971). An important development in the compartmental analysis of pollutokinetic data is the advent of physiological models, in which each compartment represents a well-defined physiological entity (Vinegar et al., 1990). Several works have placed attention on the use of physiological pollutokinetic (pharmacokinetic) models in the study of O_3 health effects (e.g., Miller et al., 1987).

Factors that may affect burden include the O_3 distribution and retention in the organs, the recirculation of O_3 between organs, and biochemical transformation. The burden variability includes contributions from both the spatiotemporal and the intersubject variabilities (in the case of O_3, the former may contribute more than the latter). One-compartment models are usually simplifications of a more complex situation, but given the paucity of data one has to work with in many cases, they provide a reasonable compromise, especially when one's final goal is a population level study. In this study, we used the stochastic one-compartment pollutokinetic model (first-order kinetics of pollutant absorption and removal processes) presented in Christakos and Hristopulos (1998). Assuming that the uptake rate is proportional to the exposure concentration, the mathematical expression of the burden $B(\boldsymbol{p})$ on a receptor $\boldsymbol{p}=(\boldsymbol{s},t)$ is given by Equation D.1 of Appendix D (e.g., in parts per million). As is shown in Equation D.1, the burden is a function of an absorption rate λ_α (e.g., in mg t^{-1} unit exposure^{-1}), a removal rate constant λ_e (t^{-1}), and the exposure map $E(\boldsymbol{p})$ obtained in a previous section. In the above model, burden provides a measure of the absorbed quantity of the pollutant over time and, thus, it may offer a more realistic estimation of the actual exposure than airborne O_3 concentration. Not all forms of burden, however, constitute a health threat. In certain cases, it is rather the biologically significant burden that is capable of changing the state of health. To estimate this kind of burden, one may then need to multiply the value obtained from Equation D.1 by a transformation fraction that is calculated experimentally (in many applications, though, this fraction is unknown and, then, it is assumed to be equal to one; Crawford-Brown, 1997). The pollutokinetic model above predicts O_3 burden levels throughout the entire receptor. More detailed pollutokinetic models can be also incorporated in the stochastic approach of Figure 1, which describes highly nonuniform burden distribution to lung tissue, transport, and chemical reactions of O_3 in the respiratory tract compartments, etc. (such models have been discussed, e.g., in Overton et al., 1987).

It is worth-noticing that Equation D.1 of Appendix D establishes a relationship between external exposure (O_3 concentration) and internal exposure (burden on target organ), which is physically meaningful as well as testable in terms of biologic monitoring (e.g., chemical concentration on body tissues or fluids). Model (D.1) has other important features that can improve considerably our scientific understanding of the human exposure processes. For example, it provides an indication of the mechanisms by which receptor exposure and organ burden are related. Also, as is shown in Christakos and Hristopulos (1998), the model can establish analytical expressions of the burden statistics (mean, covariance, etc.) in terms of the exposure and rate statistics.

Using the daily-averaged O_3 maps of Figure 3 and model (D.1), burden maps for the geographical region of eastern US are plotted for a few days during the month of July 1995 (Figure 4). For the purpose of the present simulation study, the rate values $\lambda_\alpha=0.7$ and $\lambda_e=1.0$ were assumed to derive the burden maps of Figure 4. The choice of the rate values depends on certain physiological parameters (pulmonary or alveolar ventilation, retention, volume of distribution, clearance, etc.; Droz, 1993). Typically, each set of space/time burden maps is associated with a 'representative' receptor that has specific physiological and biological characteristics (see also the discussion in the following sections). The maps of Figure 4 demonstrate the spatiotemporal variability of burden, which is the result of environmental and biological factors, acting separately as well as interacting with each other. On the basis of these

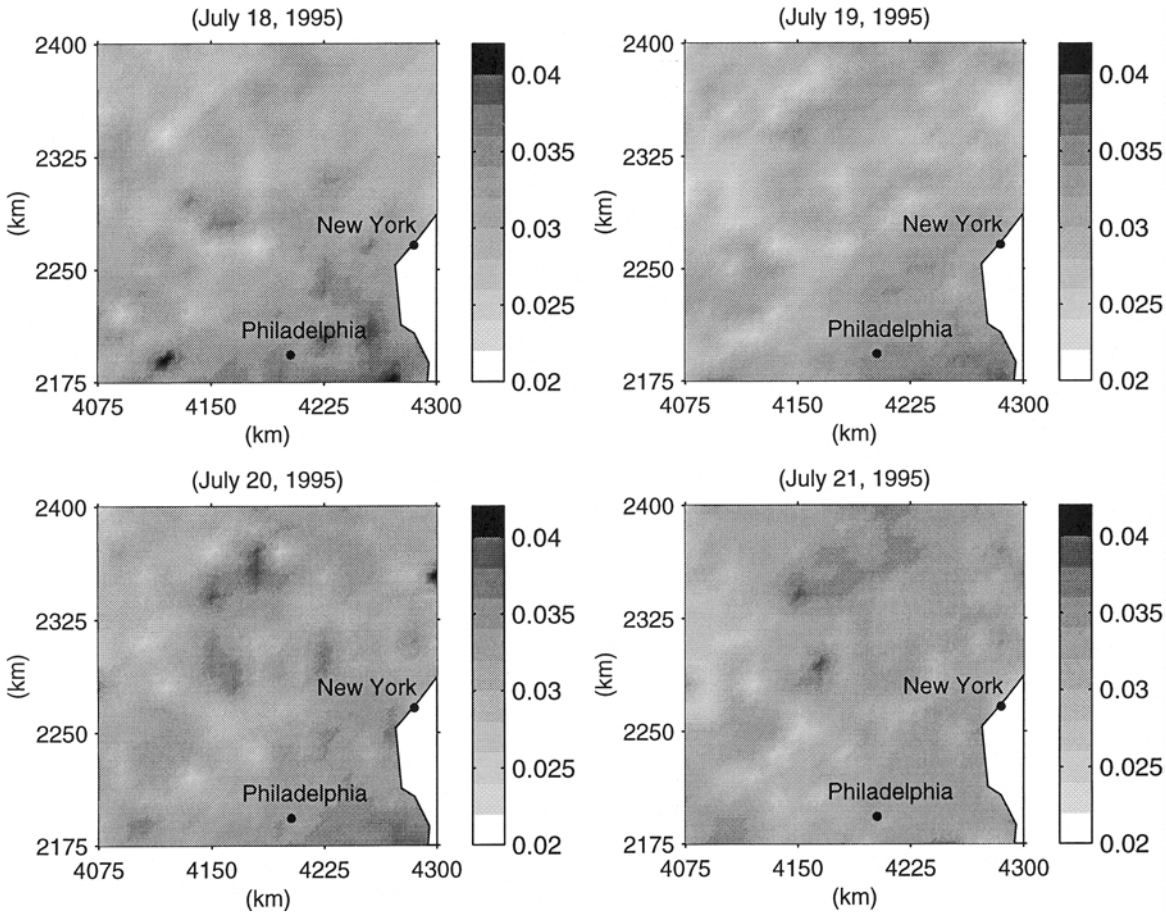

Figure 4. Maps of daily accumulated burden (ppm) on receptors at a region of eastern US.

maps, several health risk-related issues can be studied, as well. One can calculate how much of the burden on target organs could be prevented if O_3 exposures were reduced by a certain amount. Given the considerable burden variability, it is essential that the burden maps be compared with acceptable burden values. To evaluate if the human exposure is within the acceptable limits, the values of the burden maps should be compared with the appropriate health standards. The comparison should take into account intersubject and intrasubject biological variations, as well.

Furthermore, in Figures 5 and 6, temporal O_3 profiles and the associated burden profiles are shown at three specific geographical locations of the eastern US region considered above (the coordinates are shown in the figures). Monthly patterns of O_3 exposure are clearly identifiable in Figure 5. A range of λ_e-values were assumed in Figure 6 to account for uncertainty: λ_e=1.0, 0.35, and 0.06. An important concept of burden kinetics is the half-life $T_{1/2}=0.693/\lambda_e$, which is equal to the time required for burden to be reduced to 50% of its original value after uptake. The rate constant λ_e and the half-life $T_{1/2}$ are useful tools to describe how O_3 exposure variability will affect burden levels in the body. The smaller the λ_e is (or, the larger the $T_{1/2}$ is), the less affected is the burden level by changes in exposure (e.g., the longer it takes the burden to decrease when exposure ends, or to reach a steady state when exposure is stable). For $\lambda_e \geq 1.0$, the burden profile follows the daily exposure variations well and it is, therefore, a very good indicator of the exposure conditions. For $\lambda_e \leq 0.35$, burden is a rather poor indicator of the exposure fluctuations (note the differences in magnitude between burden profiles).

Semivariograms are stochastic tools that provide a quantitative assessment of exposure and burden variations. The semivariogram $\gamma_E(\tau)$, $\tau = t_2 - t_1$, of the exposure profile and the semivariogram $\gamma_B(\tau)$ of the burden profiles above are defined in Equation D.2 of Appendix D. The $\gamma_E(\tau)$ and $\gamma_B(\tau)$ functions are plotted in Figure 7. As it should be expected on the basis of the preceding analysis, when $\lambda_e \geq 1.0$, the exposure and burden semivariograms show very similar behaviors. But they start to exhibit significant differences in their shapes when $\lambda_e \leq 0.35$. The shape of the semivariograms at the origin and at large distances is of

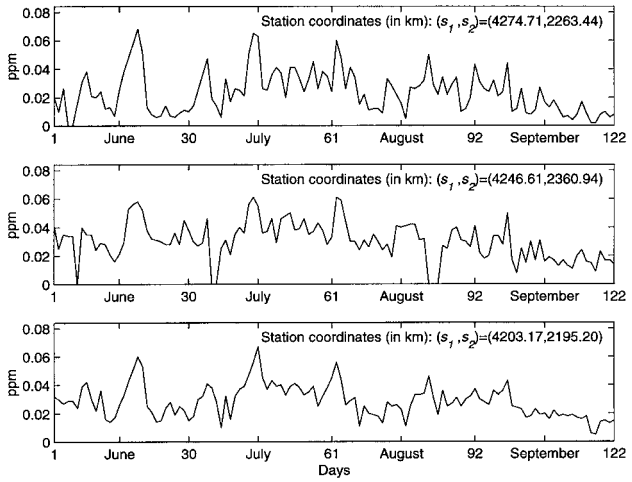

Figure 5. Daily-averaged O_3 exposure profile at three geographical locations during the period June–September 1995.

particular importance for it provides information about the behavior of the actual exposure and burden profiles. While a quadratic shape of the semivariogram at the origin implies a rather smooth temporal variation (as is the case, e.g., with λ_e=0.06), a linear shape indicates a more irregular variation exhibiting significant fluctuations (λ_e=0.35 and 1.0). An asymptotic behavior at large distances denotes a rather stationary profile fluctuating around a constant mean (λ_e=0.35 and 1.0), but a linear shape implies a nonstationary profile with temporal trends (λ_e=0.06).

Assessment of health effect and population damage

A number of studies have reported associations between O_3 exposure and health effects (e.g., exposure of humans to O_3 alters spirometric and permeability functions of the lung; Lippmann, 1989; Horvath and McKee, 1994; Simpson, 1995). The health effects can be quantified by means of an intake pathway process involving burden estimates. Burden estimates may be, indeed, more relevant in the assessment of health effects than exposure levels evaluated by airborne monitoring O_3 concentrations, because they take into consideration the pollutokinetic properties of O_3 in the body (Leung, 1991; Schulte and Perera, 1993). Physically meaningful burden–health response models may be derived at the individual receptor or at the population levels. In both cases, the relationships are stochastic, reflecting the uncertainty and the space/time variation of the human exposure variables involved.

Burden–Response Curve

Quantitative relationships needed for health risk assessment require information about the burden on the target tissue or

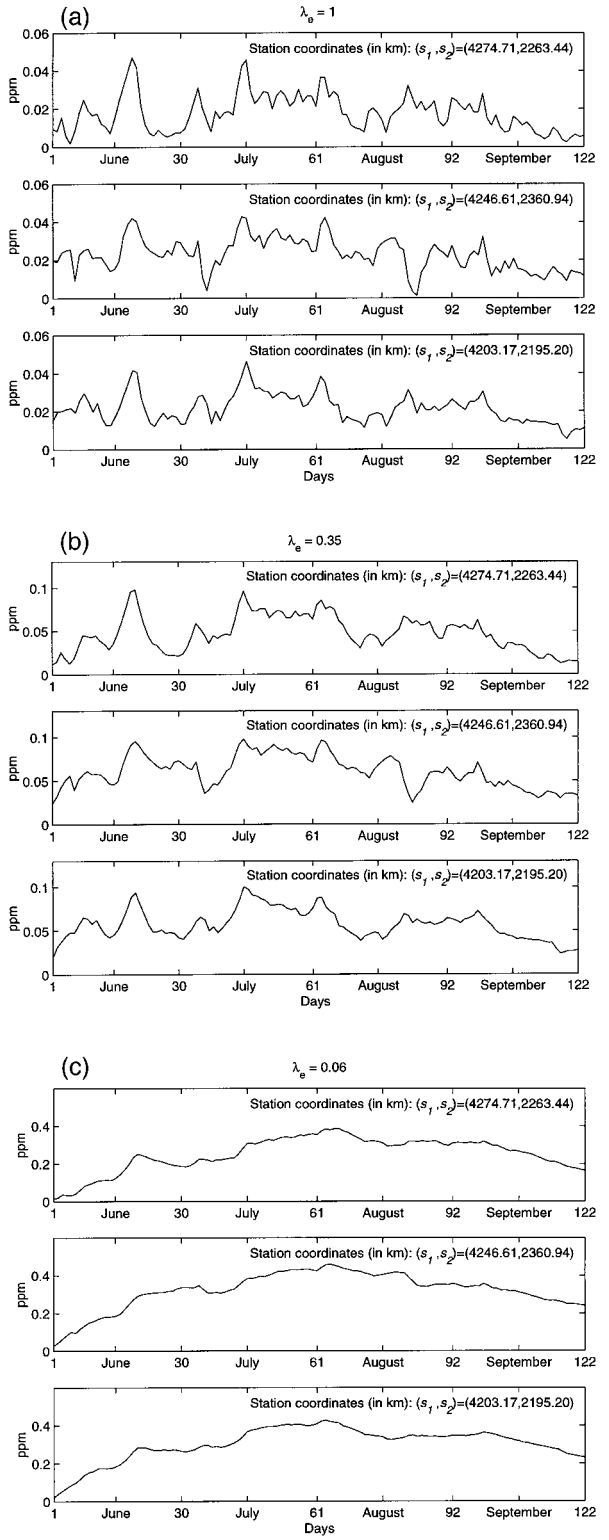

Figure 6. Burden profiles associated with the O_3 exposure profile of Figure 5: (a) λ_e = 1.0, (b) λ_e = 0.35, and (c) λ_e = 0.06.

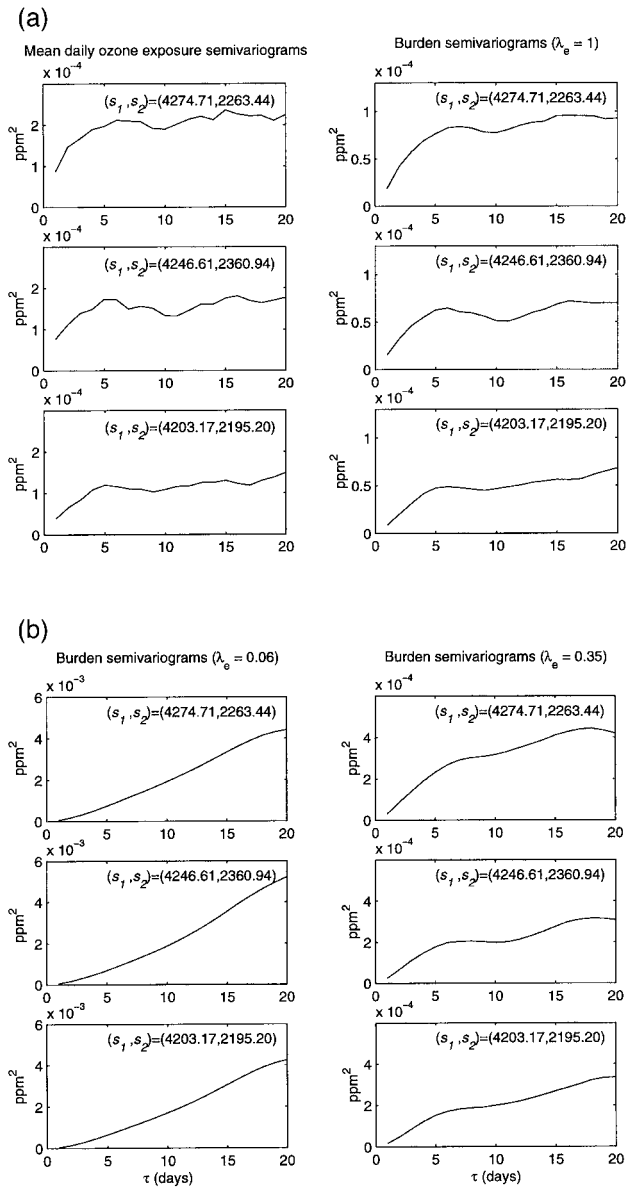

Figure 7. Semivariograms of the O_3 exposure and burden profiles of Figures 5 and 6.

organ. The expected health response or effect $H(\boldsymbol{p})$ on a receptor $\boldsymbol{p}$ due to O_3 burden $B(\boldsymbol{p})$ may be expressed as a frequency or a ratio. For example, $H(\boldsymbol{p})$ could denote the receptor's expected frequency of pulmonary function decrements (in forced expiratory volume, FEV_1; West, 1992). This frequency is usually obtained via experimental studies of control groups, in which we plot the burden on receptors vs. the percentage of receptors that exceed a specified FEV_1 level. The health effect $H(\boldsymbol{p})$ is related to the O_3 burden $B(\boldsymbol{p})$ by means of a burden–response curve $\mathcal{F}_{BR}[B,\alpha,c]$ (see Equation E.1 of Appendix E). In addition to the burden, the $\mathcal{F}_{BR}$ involves two other parameters: α, which is generally considered a random variable to indicate uncertainty, and c, which is an exponent that determines the shape of the curve (c=1, <1 and >1 are associated with linear, sublinear, and supralinear curves, respectively). The S/TRF model may offer an interpretation of the cause–effect concept underlying Equation E.1. The use of logical conditionals (e.g., $B \rightarrow H$) requires us to admit various possible realizations besides the actual (but unknown) one. Then, burden B may be considered—from a stochastic standpoint—as being a cause of the effect H if both B and H occur in the observed realization, but in the vast majority of the other realizations in which B does not occur, H does not occur either.

By taking into consideration the external exposure–internal exposure relationship introduced in Equation D.1 of Appendix D, the $\mathcal{F}_{BR}$ model (E.1) may be linked to existing empirical exposure–response relationships (like these discussed, e.g., in McKee, 1994). It is noteworthy, however, that when using the empirical exposure–response relationships, much of the observed variation in the response may be due to the use of ambient O_3 concentration as a surrogate for the actual burden on target tissues (Hu et al., 1992). This is a problem that can be avoided by using the burden–response model (E.1) instead of the empirical exposure–response relationship. Equation E.1 may be assumed valid for any receptor that belongs to a specific cohort (i.e., a group of individuals with similar time/activity profiles). Indeed, in addition to the burden on the target organs, a number of cohort-related factors can potentially affect α and c (e.g., Hazucha, 1993; Rombout and Schwarze, 1995). These factors include: the exposure duration τ_e [short term (1–3 h), prolonged ($\geq$6–8 h), and long-term (months or years) exposures are associated with different kinds of health effects]; the activities of the receptors during exposure (respiratory effects may occur at increased exertion levels, even at low O_3 exposure levels); pre-existing conditions (e.g., receptors with pre-existing limitations in pulmonary function may experience respiratory problems with greater clinical significance than healthy individuals); biological and physiological characteristics; and age group of the receptors (older persons are more sensitive to O_3 exposure than young adults). In view of the considerable uncertainty implied by all the above factors, stochastic analysis represents the variables of Equation E.1 in terms of random fields. The stochastic analysis may involve the pdf of each one of the above cohort factors (the exposure duration pdf, the activity pdf, etc.), thus generating a set of possible values for α and c. These pdf may be obtained from field studies and/or the literature.

Mapping of Population Health Damage Indicators

The exposure conditions having been mapped in space/time and related to burden on the body, and the expected health effect on an individual receptor been quantified, the health

damage on a community-wide basis needs to be assessed in terms of health damage indicators. These indicators are a prerequisite for environmental health policy and management studies.

A simple population damage indicator $\Psi_v(\boldsymbol{p})$ is the average local health damage to the population of the region $v(\boldsymbol{s})$ at time t due to the health response $H(\boldsymbol{p})$. The $\Psi_v(\boldsymbol{p})$ is defined by the response–damage relationship of Equation E.2 of Appendix E, and is a function of the density $\Theta(\boldsymbol{p})$ of receptors in the neighborhood of $v(\boldsymbol{s})$. The physical significance of the local damage $\Psi_v(\boldsymbol{p})$ depends on the human health effect considered. If, e.g., $H(\boldsymbol{p})$ is the frequency (in percentage) of physiologic decrements in the population of the region $v(\boldsymbol{s})$, the $\Psi_v(\boldsymbol{p})$ will denote the expected number of people with such problems in the region (e.g., number of receptors affected/km^2). From the population damage, a useful normalized local damage indicator $\psi_v(\boldsymbol{p})$ (dimensionless) can be defined as the ratio of $\Psi_v(\boldsymbol{p})$ over the average damage $\Psi_V(t)$ occurred at the global region V (see Equation E.3 of Appendix E), $[V \supset v(\boldsymbol{s})]$. The $\psi_v(\boldsymbol{p})$ may be, e.g., the ratio of the anticipated local number of incidents per unit area (people affected by O_3 exposure in a specific county) over the anticipated global number of incidents per unit area within the entire eastern US.

A possible health damage scenario for the eastern US geographical region V considered in the previous sections is simulated next. The values $c=0.5$ and 1.5 were assumed for the exponent of Equation E.1, i.e., both sublinear and supralinear curves were used. These seem to be reasonable choices given that several studies have shown that during the period of intense exposure, damage is usually a nonlinear function of burden (e.g., Rappaport, 1991). Furthermore, it was assumed that $\alpha(\boldsymbol{p})$ is randomly varying within the interval 1.63 ± 0.05 for the sublinear model and the interval 7.25 ± 0.25 for the supralinear model. These intervals account for the contribution of geographical and temporal variabilities on the health effect. The population density values were calculated on the basis of data obtained from the US Bureau of Census (1992). Ozone exposure and health damage analyses were carried out at an observation scale that is consistent with the domain $v(\boldsymbol{s})$ at which the damage variables are observed. The mapping grid size was selected on the basis of the area statistics of the counties. Under these conditions, maps of the population damage indicator Ψ_v (number of receptors affected/km^2) are plotted in Figure 8. The Ψ_v varies in space and time. Note the considerable effect of the different burden–health response curves assumed ($c=0.5$ vs. $c=1.5$). As was the case with similar exposure studies in the past, the Ψ_v pattern is expected to be driven significantly by the population distribution. Areas where exposure has the highest probability to cause adverse health effects at the local population level can be detected with the help of the Ψ_v maps. Furthermore, a map of the normalized damage indicator ψ_v is plotted in Figure 9. Unlike the Ψ_v maps, the ψ_v maps may be not affected significantly by the shape of the burden–response curve, for the latter appears in both the nominator and the denominator of Equation E.3. Interpreted with judgment (i.e., keeping in mind the assumptions made above concerning the exposure, biological, and health response parameters, the cohort characteristics, etc.), the maps of Figures 8 and 9 may offer valuable insight regarding the possible distribution of health damage on the population due to O_3 exposure. For example, the population

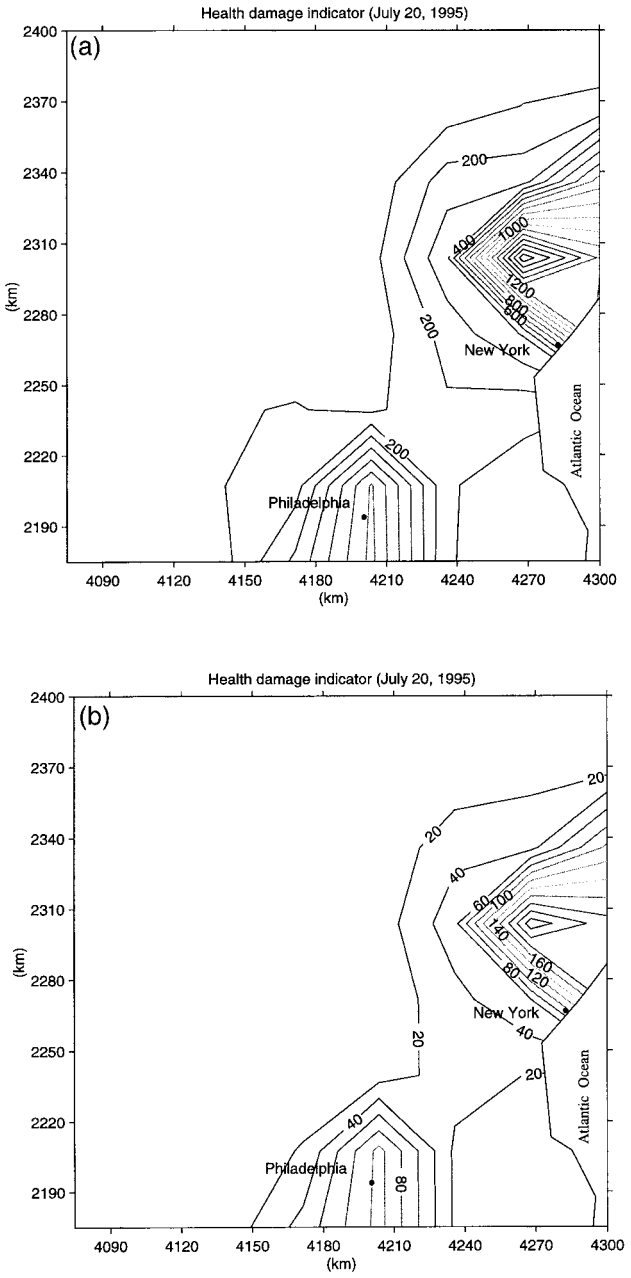

Figure 8. Map of the health damage indicator Ψ_v (number of receptors affected/km^2) on July 20: (a) for $c=0.5$ and (b) for $c=1.5$.

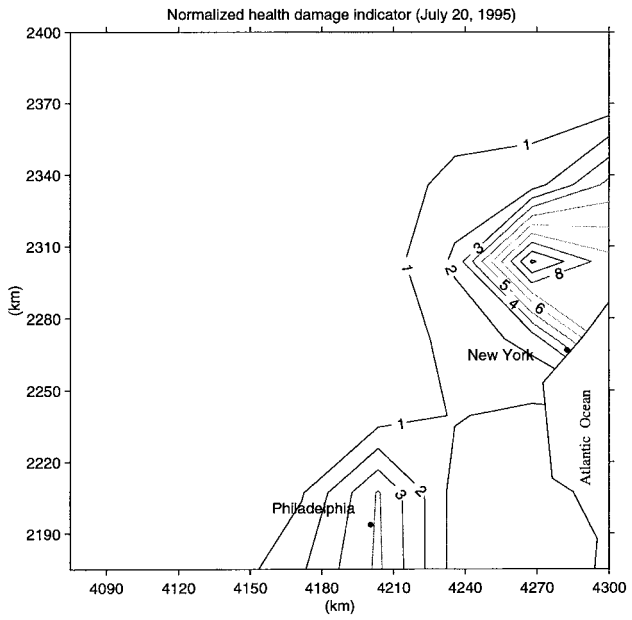

Figure 9. Map of the normalized health damage indicator ψ_υ (dimensionless) on July 20 for $c = 0.5$.

health damage at a local area with $\psi_\upsilon = 5$ is expected to be five times larger than the average damage of the entire region V, for a population of receptors belonging to a specified cohort.

While the burden maps represent the actual exposure an individual 'representative' receptor that belongs to a specific cohort may receive in space/time, the damage maps assess the absolute or relative impact of exposure on the population as a whole. This is, clearly, due to the effect of the population density. It may happen, e.g., that while the area $\upsilon(\boldsymbol{s}_1)$ shows higher burden levels (at the receptor's level) than the area $\upsilon(\boldsymbol{s}_2)$, it nevertheless experiences relatively smaller damage (at the population level) than $\upsilon(\boldsymbol{s}_2)$, due to its smaller population density. In other words, the population damage maps possess a social policy dimension that burden maps may have not.

The sequence of maps (exposure, burden, and health damage) presented above (Figures 3–9) provides the means to consider human exposure as a spatiotemporal system, by looking at the whole picture—not just certain isolated parts. Exposure, burden and health effects are considered in a spatiotemporal continuum, which previous statistical studies did not allow (e.g., maps of purely spatial exposure variability were studied by Hayes et al., 1988). Moreover, Christakos and Vyas (1998a) have shown that spatiotemporal mapping can be considerably more accurate than purely spatial mapping. By comparing possible exposure maps with the corresponding population damage maps, functional relationships may be identified and regulatory standards analyzed in a probabilistic context.

Discussion

Human exposure assessment to potentially harmful pollutants is an important area from both the scientific research and the health management standpoints. In earlier papers (Christakos and Vyas, 1998a and 1998b), a method was developed for studying the health effects of spatiotemporal O_3 exposure on human populations. Among the improvements of the present work over these earlier studies are the derivation of the previous exposure mapping method as a special case of a more general and powerful (BME) analysis, the incorporation of pollutokinetic modelling in spatiotemporal health effect analysis and mapping, and the consideration of nonlinear burden–response curves with random coefficients.

The proposed approach relies on a conceptual model that describes human exposure as a sequence of space/time maps related to airborne exposure concentration, burden, health effect, and population damage. This is a holistic perspective that looks at the whole picture of human exposure assessment—not only certain isolated parts. Holisticity introduces an implicit theory of meaning as well as a theory of knowledge. The unit of meaning is not a single part, but rather a whole system of parts, which are interlinked and interrelated in various ways. From an epistemological viewpoint, holisticity holds that single hypotheses about human exposure are not tested in isolation, but rather as parts of larger complexes (examples of such complexes are the environmental health paradigms; Christakos and Hristopulos, 1998).

The holistic perspective reveals important functional relationships between O_3 exposure and subsequent burden, health effect, and population damage. Key to studying these relationships is the quantitative assessment of human exposure variability in the space/time continuum. Random field models—which rigorously represent the uncertainty, variability, and imperfect knowledge characterizing most human exposure variables—presuppose a continuum of space/time points and then attribute the values of the human exposure variables to these points. The space/time continuum is not coherent in the abstract mathematical sense; it rather enforces coherence by means of empirical investigations. The choice of a space/time geometry must avoid discrepancies between the natural geometry—as revealed by physical knowledge—and the appropriate mathematical geometry.

Composite space/time exposure maps are obtained using BME analysis. From the BME mapping viewpoint, the issue is not merely how to deal with data, but also how to interpret and integrate them into the understanding process. In a sense, this expands the study domain to include the observer (environmental modeller) as well as the observed (exposure distribution). The air monitoring method of determining exposure to O_3 has certain limitations, which in many cases

prevent it from offering a realistic assessment of the actual exposure a target organ has received. In this work, pollutokinetic models have been used to overcome some of these limitations. Although rather simple, one-compartment pollutokinetics can offer an accurate representation of the fate of the pollutant within the body. Inputs to the pollutokinetic equation are the O_3 exposure map and the physiological/biological features of the receptor, and its output is the space/time burden map. Each of these maps is associated with a 'representative' receptor and its interpretation should take into account important intersubject and intrasubject biological variations. The burden map is, in turn, related to the population health damage via an integral operation that accounts for the burden–response association and the population density distribution. Other factors—such as exposure duration, activities, and pre-existing conditions of the receptors, biological and physiological characteristics and age groups—are taken into consideration in the development of the burden–response curve. Health damage maps are useful for generating or testing hypotheses regarding the etiology of health deterioration (e.g., in terms of O_3 or other pollutants acting in synergy). The maps are essential tools in the evaluation of alternative health management strategies with respect to efficiency, cost, etc.

While the burden distribution B implies the existence of the active form of the pollutant in target organs or tissues, it is the dose rate D_r which determines the interaction rate between the biologically active form and target organs and tissues. The cumulative dose or simply dose D is the cumulative quantity of the biologically active form delivered to the receptor during the time period τ_d in which interactions between the biologically active form and target organs or tissues take place. The τ_d may be larger than the exposure duration, because biologically active pollutants are retained in the body even after exposure is terminated. Unfortunately, in many cases, the τ_d is not known, which means that the dose cannot be calculated. The rigorous incorporation of the dose distribution in stochastic human exposure modelling requires parallel advances in experimental techniques for determining D_r and D.

A significant part of the present work was concerned with aspects of scientific methodology. Indeed, given the paucity of data (physiological, biochemical, etc.), certain assumptions had to be made regarding the values of the parameters of the pollutokinetic, burden–response, etc., models. Maps describing possible distributions of exposure, burden, and health damage were produced, which should be interpreted in the light of the above assumptions. Indeed, as already mentioned, each set of maps may be associated with a 'representative' receptor that belongs to a specific cohort. Each set of maps can help the interested health scientist or administrator derive conclusions about the expected exposure effects for a specific cohort. Different cohorts should be associated with different sets of maps. Addressing itself principally to the scientific business of spatiotemporal human exposure mapping, this work does not necessarily endorse any specific exposure standards. The proposed method is best viewed as a tool for the investigator that may offer a useful description of the human exposure data and an important basis for further analysis.

Acknowledgments

This work has been supported by grants from the Department of Energy (Grant no. DE-FC09-93SR18262), the Army Research Office (Grant no. DAAG55-98-1-0289), and the National Institute of Environmental Health Sciences (Grant no. P42 ES05948-02).

References

Choi K.-M., Christakos G., and M.L. Serre. Recent developments in vectorial and multi-point Bayesian maximum entropy analysis. In *IAMG98, Proceed. of 4th Annual Confer. of the Internat. Assoc. for Mathematical Geology-Vol. 1*, Buccianti A., G. Nardi and R. Potenza (eds.), 91-96, De Frede Editore, Naples, Italy, 1998.

Christakos G. Random Field Models in Earth Sciences. Academic Press, San Diego, CA, 1992, 474 pp.

Christakos G. While God is raining brains, are we holding umbrellas? The role of Modern Geostatistics in spatiotemporal analysis and mapping. Keynote lecture. In *IAMG98, Proceed. of 4th Annual Confer. of the Internat. Assoc. for Mathematical Geology-Vol. 1,* Buccianti A., G. Nardi and R. Potenza (eds.), 33-53, De Frede Editore, Naples, Italy, 1998.

Christakos G. Modern geostatistics in the analysis of spatiotemporal environmental data: the BME approach. Short Course Notes, IAMG98, Ischia, Italy, 1998.

Christakos G., and Hristopulos D.T. Spatiotemporal Environmental Health Modelling: A Tractatus Stochasticus. Kluwer Acad. Publ., Boston, MA, 1998, 423 pp.

Christakos G., and Vyas V. A composite spatiotemporal study of ozone distribution over eastern United States. *Atmospheric Environment* 1998: 32 (16): 2845–2857.

Christakos G., and Vyas V. A novel method for studying population health impacts of spatiotemporal ozone distribution. *Soc. Sci. Med.* 1998: 47 (8): 1051–1066.

Crawford-Brown D.J. Theoretical and Mathematical Foundations of Human Health Risk Analysis. Kluwer Acad. Publ., Boston, Massachusetts, 1997, 208 pp.

Droz P.O. Biologic monitoring and pharmacokinetic modelling for the assessment of exposure. In: Schulte P.A., and Perera, F.P. (Eds.), Molecular Epidemiology. Academic Press, San Diego, CA, 1993, pp. 137–157.

Hayes S.R., Austin B.S., and Rosenbaum A.S. A technique for assessing the effects of ROG and NO_x reductions on acute ozone exposure and health risk in the south coast air basin. Systema Applications, San Rafael, CA, 1988.

Hazucha M.J. Meta-analysis and 'effective dose' revisited. In: U. Mohr, et al. (Eds.), Advances in Controlled Clinical Inhalation Studies. Springer-Verlag, Berlin, Germany, 1993, pp. 247–256.

Horvath S.M., and McKee D.J. Health risk assessment of ozone. In: McKee, D.J. (Ed.), Tropospheric Ozone: Human Health and Agricultural Impacts. Lewis Publ., Boca Raton, FL, 1994, pp. 39–83.

Hu S.C., Ben-Jebria A., and Ultman J.S. Longitudinal distribution of ozone absorption in the lung: quiet respiration in healthy subjects. *J. Appl. Physiol.* 1992: 73: 1655–1661.

Leung H.-W. Development and formulation of physiologically-based pharmacokinetic models for toxicological applications. *J. Toxicol. Environ. Health* 1991: 32: 247–267.

Lippmann M. Health effects of ozone: a critical review. *J. Air Pollut. Control Assoc.* 1989: 39: 672–695.

Logan J.A. Ozone in rural areas of the US. *J. Geophys. Res.* 1989: 94 (D6): 8511–8532.

McCurdy T.R. Human exposure to ambient ozone. In: McKee, D.J. (Ed.), Tropospheric Ozone: Human Health and Agricultural Impacts. Lewis Publ., Boca Raton, FL, 1994, pp. 85–127.

McDonnell W.F., Horstman D.H., Hazucha M.J., Seal E., Haak E.D., Salaam S.A., and House D.E. Pulmonary effects of ozone exposure during exercise: dose–response characteristics. *J. Appl. Physiol.* 1983: 54: 1345–1352.

McKee D.J. (Ed.). Tropospheric Ozone: Human Health and Agricultural Impacts. Lewis Publ., Boca Raton, FL, 1994.

Miller F.D., Overton J.H. Jr., Smolko E.D., Graham R.C., and Menzel D.B. Hazard assessment using an integrated physiologically based dosimetry modelling approach: ozone. Pharmacokinetics in Risk Assessment, Vol. 8. National Academy Press, Washington, DC, 1987, pp. 353–368.

Overton J.H. Jr., Graham R.C., and Miller F.J. Mathematical modelling of ozone absorption in the lower respiratory tract. Pharmacokinetics in Risk Assessment, Vol. 8. National Academy Press, Washington, DC, 1987, pp. 303–311.

Piotrowski J. The Application of Metabolic and Excretion Kinetics to Problems of Industrial Toxicology. National Institute of Health, Washington DC, 1971, 166 pp.

Rappaport S.M. Exposure assessment strategies. In: Rappaport, S.M., and Smith, T.J. (Eds.), Expos. Assess. Epidemiol. Haz. Control. Lewis Publ., Chelsea, MI, 1991, pp. 219–249.

Rombout P.J.A., and Schwarze P.E. Quantitative exposure–response relationships for ozone. Proc. of the Nordic Expert Meet. on the Estimation of Potential Health Effects from Air Pollut. Exposure on a Regional Scale, Oslo, Norway, October 15–17, 1995.

Ryan P.B. An overview of human exposure modelling. *J. Exposure Anal. Environ. Epidemiol.* 1991: 1 (4): 453–474.

Schulte P.A., and Perera F.P. (Eds.). Molecular Epidemiology. Academic Press, San Diego, CA, 1993, 588 pp.

Serre M.L., Bogaert P., and Christakos G. Computational investigations of Bayesian maximum entropy spatiotemporal mapping. Proc. of IAMG98 Confer. on Time–Space Systems in Geology and Environmental Sciences, Ischia, Italy, 1998.

Simpson D. Modelled ozone concentrations in relation to health issues. Proc. of the Nordic Expert Meet. on the Estimation of Potential Health Effects from Air Pollut. Exposure on a Regional Scale, Oslo, Norway, October 15–17, 1995.

Taylor A.C. Using objective and subjective information to develop distributions for probabilistic exposure assessment. *J. Exposure Anal. Environ. Epidemiol.* 1993: 3 (3): 285–298.

Thurston G.D., Ito K., Kinney P.L., and Lippmann M. A multi-year study of air pollution and respiratory hospital admissions in three New York State metropolitan areas: results for 1988 and 1989 Summers. *J. Exposure Anal. Environ. Epidemiol.* 1992: 2 (4): 429–450.

US Bureau of Census. 1990 Census of Population and Housing, Summary Tape File 1-C. US Department of Commerce, Bureau of Census, Washington, DC, 1992.

Vinegar A., Winsett D.W., Andersen M.E., and Conolly R.B. Use of physiologically-based pharmacokinetic model and computer simulation for retrospective assessment of exposure to volatile toxicants. *Inhalation Toxicol.* 1990: 2: 119–128.

West, J.B. Pulmonary Pathophysiology, 5th edn. Williams and Wilkins, Baltimore, Maryland, 1992.

Appendix A

The usual physical knowledge available in many applications is the exposure covariance function $c_E(\boldsymbol{h},\tau)=\exp(-\boldsymbol{h}^2/a^2-\tau^2/b^2)$, where a and b are correlation coefficients determined from the data, $\boldsymbol{h}^2=(\boldsymbol{s}_2-\boldsymbol{s}_1)^2$ and $\tau^2=(t_2-t_1)^2$. A geometric metric that is consistent with the empirical covariance above is of the form $|\boldsymbol{p}| = \sqrt{\boldsymbol{h}^2 + a^2\tau^2/b^2}$.

The basic BME exposure equations are as follows (Christakos, 1998b):

$$\overline{g_\alpha}(\boldsymbol{p}_{\rm map}) = \int d\,\varepsilon_{\rm map} g_\alpha(\varepsilon_{\rm map}) \exp \mathcal{Y}_{\mathcal{G}}[\varepsilon_{\rm map};\boldsymbol{p}_{\rm map}], \quad \alpha = 0, 1, \ldots, N_c, \tag{A.1}$$

and

$$\frac{\partial}{\partial\varepsilon_\ell}\mathcal{Y}_{\mathcal{S}}\{\varepsilon_{\rm soft}, \exp \mathcal{Y}_{\mathcal{G}}[\varepsilon_{\rm map};\boldsymbol{p}_{\rm map}]\}_{\varepsilon_\ell=\hat{\varepsilon}_\ell} = 0. \tag{A.2}$$

BME analysis also provides the *a posteriori* (probability density function) that incorporates the total knowledge $\mathcal{K}$, i.e.,

$$f_{\mathcal{K}}(\varepsilon_k) = \mathcal{Y}_{\mathcal{S}}\{\varepsilon_{\rm soft}, \exp \mathcal{Y}_{\mathcal{G}}[\varepsilon_{\rm map};\boldsymbol{p}_{\rm map}]\}, \tag{A.3}$$

where $\varepsilon_{\rm map}=(\varepsilon_{\rm data},\ \varepsilon_\ell)$.

Appendix B

At each geographical location, the temporally averaged 1-h O_3 exposure $E(\boldsymbol{p})$ is calculated by:

$$E(\boldsymbol{p}) = |\tau_e(\boldsymbol{p})|^{-1} \int_{\tau_e(\boldsymbol{p})} dt' f_e(\boldsymbol{s}, t-t') E_{1-h}(\boldsymbol{s}, t-t'), \tag{B.1}$$

where $\tau_{\rm e}$ is the exposure duration (in hours) during each day, and $f_{\rm e}$ is the exposure frequency (in percentage), i.e., the fraction of total exposure time during which the receptor is actually exposed.

Appendix C

A metrical structure is defined for the exposure space/time continuum that includes a spatial distance $|\boldsymbol{h}| = \sqrt{(\boldsymbol{s}_2 - \boldsymbol{s}_1)^2}$ and an independent time interval $\tau = t_2 - t_1$. Ozone exposure is represented in terms of the S/TRF-ν/μ model with a generalized spatiotemporal covariance of the form of (Christakos, 1992):

$$k_E(|\boldsymbol{h}|,\tau) = c\delta(|\boldsymbol{h}|)\delta(\tau) + \boldsymbol{A}^{\mathrm{T}}\boldsymbol{T}\delta(|\boldsymbol{h}|) + \boldsymbol{B}^{\mathrm{T}}\boldsymbol{R}\delta(\tau) + \boldsymbol{R}^{\mathrm{T}}\boldsymbol{\Gamma}\boldsymbol{T}, \tag{C.1}$$

where $\boldsymbol{R} = \{|\boldsymbol{h}|^{2\nu+1}\}_{\nu=0,1,2}$; $\boldsymbol{T} = \{\tau^{2\mu+1}\}_{\mu=0,1,2}$; the $\boldsymbol{A} = \{(-1)^{\mu+1}a_\mu\}_{\mu=0,1,2}$; $\boldsymbol{B} = \{(-1)^{\nu+1}b_\nu\}_{\nu=0,1,2}$‘ and $\boldsymbol{\Gamma} = \{(-1)^{\nu+\mu}a_{\nu\mu}\}_{\nu,\mu=0,1,2}$ are vectors and matrix of known coefficients. Other possible models are discussed in Christakos and Hristopulos (1998).

Appendix D

Assuming that the uptake rate is proportional to the exposure concentration, the burden on a receptor $\boldsymbol{p} = (\boldsymbol{s},t)$ is given by (in parts per million):

$$B(\boldsymbol{p}) = \begin{cases} \int_0^t dt' \lambda_\alpha(\boldsymbol{s},t') E(\boldsymbol{s},t') \exp(-\zeta_t + \zeta_{t'}), & \text{during exposure } (t \le t_0) \\ B(\boldsymbol{s},t_0)\exp(-\zeta_t), & \text{after exposure } (t > t_0) \end{cases}, \tag{D.1}$$

where $\zeta_t = \int_0^t \mathrm{d}\tau \lambda_{\mathrm{e}}(\boldsymbol{s},\tau)$; λ_α is the absorption rate, λ_{e} is the removal rate constant, and $E(\boldsymbol{p})$ denotes the O_3 exposure map.

The semivariograms of the exposure and burden profiles are defined by, respectively:

$$\left.\begin{aligned} \gamma_E(\tau) &= \tfrac{1}{2}\overline{[E(t+\tau) - E(t)]^2} \\ \gamma_B(\tau) &= \tfrac{1}{2}\overline{[B(t+\tau) - B(t)]^2} \end{aligned}\right\}. \tag{D.2}$$

Appendix E

Ozone burden $B(\boldsymbol{p})$ and health effect $H(\boldsymbol{p})$ are assumed to be related by a burden–response curve of the form:

$$H(\boldsymbol{p}) = \mathcal{F}_{BR}[B] = \alpha(\boldsymbol{p})B^c(\boldsymbol{p}), \tag{E.1}$$

where $\alpha(\boldsymbol{p})$ is a random variable to indicate uncertainty, and the exponent c determines the shape of the curve.

The population damage indicator $\Psi_\upsilon(\boldsymbol{p})$ is the average local health damage to the population of the region $\upsilon(\boldsymbol{s})$ at time t due to the health response $H(\boldsymbol{p})$ of Equation E.1. The $\Psi_\upsilon(\boldsymbol{p})$ is defined by the response–damage relationship:

$$\Psi_\upsilon(\boldsymbol{p}) = |\upsilon(\boldsymbol{s})|^{-1} \int_{\upsilon(\boldsymbol{s})} d\boldsymbol{s}' \theta(\boldsymbol{s} - \boldsymbol{s}', t) H(\boldsymbol{s} - \boldsymbol{s}', t), \tag{E.2}$$

where $\theta(\boldsymbol{p})$ is the density of receptors in the neighborhood of $\upsilon(\boldsymbol{s})$. A useful normalized local damage indicator can be, also, defined as follows (dimensionless):

$$\psi_\upsilon(\boldsymbol{p}) = \Psi_\upsilon(\boldsymbol{p})/\Psi_V(t), \tag{E.3}$$

where $\Psi_V(t) = V^{-1}\int_V \mathrm{d}\boldsymbol{s}\theta(\boldsymbol{p})H(\boldsymbol{p})$ is the average damage over the global region V [where $V \supset \upsilon(\boldsymbol{s})$].